Acidic environments trigger intracellular H^+-sensing FAK proteins to re-balance sarcolemmal acid-base transporters and auto-regulate cardiomyocyte pH

Abigail D. Wilson[1], Mark A. Richards[1], M. Kate Curtis[1], Mala Rohling[1], Stefania Monterisi[1], Aminah A. Loonat[1], Jack Miller[1,2,3], Vicky Ball[1], Andrew Lewis[3], Damian Tyler[1,3], Anna Moshnikova[4], Oleg A. Andreev[4], Yana K. Reshetnyak[4], Carolyn Carr[1], Pawel Swietach[1]

1) Department of Physiology, Anatomy & Genetics, University of Oxford, Sherrington Building, Parks Road, OX1 3PT, Oxford, England
2) Department of Physics, Clarendon Laboratory, University of Oxford, Oxford, OX1 3PU
3) Oxford Centre for Clinical Magnetic Resonance Research (OCMR), Radcliffe Department of Medicine, Level 0, John Radcliffe Hospital, Headington, Oxford, OX3 9DU
4) Physics Department, University of Rhode Island, 2 Lippitt Rd, Kingston, RI 02881, USA

**Corresponding author.* Email: pawel.swietach@dpag.ox.ac.uk ; Department of Physiology, Anatomy & Genetics, Sherrington Building, Parks Road, OX1 3PT, Oxford, England.

Short title: Auto-regulation of cardiomyocyte pH control

Word count: 8935

Category: Original Article

Keywords: Acidity; Cardiomyocyte; Homeostasis; pH sensor; Ischemia

ABSTRACT

AIMS: In cardiomyocytes, acute disturbances to intracellular pH (pHi) are promptly corrected by a system of finely-balanced sarcolemmal acid-base transporters. However, these fluxes become thermodynamically re-balanced in acidic environments, which inadvertently causes their set-point pHi to fall outside the physiological range. It is unclear whether an adaptive mechanism exists to correct this thermodynamic challenge and return pHi to normal.

METHODS AND RESULTS: Following left-ventricle cryo-damage, a diffuse pattern of low extracellular pH (pHe) was detected by acid-sensing pHLIP. Despite this, pHi measured in the beating heart (^{13}C NMR) was normal. Myocytes had adapted to their acidic environment by reducing Cl^-/HCO_3^- exchange (CBE)-dependent acid-loading and increasing Na^+/H^+ exchange (NHE1)-dependent acid-extrusion, as measured by fluorescence (cSNARF1). The outcome of this adaptation on pHi is revealed as a cytoplasmic alkalinisation when cells are superfused at physiological pHe. Conversely, mice given oral bicarbonate to improve systemic buffering had reduced myocardial NHE1 expression, consistent with a needs-dependent expression of pHi-regulatory transporters. The response to sustained acidity could be replicated *in vitro* using neonatal ventricular myocytes (NRVMs) incubated at low pHe for 48 h. The adaptive increase in NHE1 and decrease in CBE activities was linked to *Slc9a1* (NHE1) upregulation and *Slc4a2* (AE2) downregulation. This response was triggered by intracellular H^+ ions because it persisted in the absence of CO_2/HCO_3^- and became ablated when acidic incubation media had low chloride concentration, a manoeuvre that reduces the extent of pHi decrease. Pharmacological inhibition of FAK-family non-receptor kinases, previously characterised as pH-sensors, ablated pHi autoregulation. In support of a pHi-sensing role, FAK protein Pyk2 (auto)phosphorylation was reduced within minutes of exposure to acidity, ahead of adaptive changes to pHi control.

CONCLUSIONS: Cardiomyocytes fine-tune the expression of pHi-regulators so that pHi is at least 7.0. This autoregulatory feedback mechanism defines physiological pHi and protects it during pHe vulnerabilities.

TRANSLATIONAL PERSPECTIVE

As a consequence of the inherent thermodynamic coupling between intra- and extracellular pH (pHi/pHe), sustained changes to perfusion, such as those in coronary disease or development, would have deleterious effects on the internal acid-base milieu of myocytes and hence cardiac function, unless offset by a corrective process. Using *in-vivo* and *in-vitro* models of acidification, we characterise this adaptive process functionally, and describe how it is engaged to auto-regulate pHi. This additional layer of homeostatic oversight enables the myocardium to operate within its optimal pHi-range, even at times when vascular perfusion is failing to maintain chemical constancy of the interstitial fluid.

INTRODUCTION

As a result of an exquisite pH-sensitivity of protein function, many cardiac signalling pathways operate effectively only over a narrow range of intracellular pH (pHi) centred around 7.1-7.2[1,2]. Disturbances that push pHi outside this range have been documented to cause contractile depression[3-7], aberrant Ca^{2+} handling[7,8] and trigger electrical arrhythmias[9]. To control pHi, cardiomyocytes are equipped with a system of H^+-equivalent transporters[10-14], including Na^+/H^+ exchanger-1 (NHE1; *SLC9A1*)[15,16], electrogenic Na^+-HCO_3^- cotransporter (NBCe1; *SLC4A4*)[17-20], electroneutral Na^+-HCO_3^- cotransporter (NBCn1; *SLC4A7*)[18,19,21] and Cl^-/HCO_3^- exchangers (CBE; *SLC4A1-3*[18,22,23] and *SLC26A6*[24-26]). This system regulates pHi towards a set-point, at which the H^+-equivalent flux carried by acid-extruders (NHE1, NBCs) balances the flux carried by acid-loaders (CBE). According to the canonical model, this regulatory system is sufficient to maintain a favourable pHi; for example, in response to an untoward cytoplasmic acid-load, intracellular H^+ ions allosterically activate acid-extruders and inhibit acid-loaders, thereby restoring pHi within minutes. However, an inherent property of the proteins' transport-cycle is that extracellular pH (pHe) also influences activity[24,27,28]. As a result, extracellular acidosis inhibits acid-extruders and activates acid-loaders thermodynamically, thereby driving pHi to a lower level. Without a corrective mechanism, the internal acid-base milieu would become subservient to extracellular conditions, which is problematic because the interstitial fluid is susceptible to pH fluctuations, such as those arising from changes in perfusion during vascular development or disease[29-31]. This regulatory flaw raises two questions: *(1)* is the cardiomyocyte able to offset thermodynamic pHe-pHi coupling and maintain internal homeostasis irrespective of the external milieu, i.e. is there a secondary level of pHi oversight that would be critical at times of reduced or aberrant vascular perfusion, and *(2)* what instructs the pHi-regulatory apparatus to assemble in a way that produces a desired set-point, i.e. how does a cardiomyocyte determine what is normal pHi?

A plausible means of offsetting the undesirable coupling between pHe and pHi may involve an adaptive change to the expression of pHi regulators, but how this takes place is unclear. Indeed, most of our understanding of how pHi regulators are controlled relates to their post-translational status[32-38], i.e. a more acute and labile

response that does not operate in the format of a pHi feedback circuit. A corrective mechanism would require an intracellular H^+-sensor to instruct the appropriate expression of transporter-coding genes, but its identity in the heart is not established. Several candidates for such a sensor exist, including histone (de)acetylase enzymes[39] and the non-receptor kinases FAK1[40] and FAK2 (also called Pyk2)[41,42]. Additionally, soluble adenylyl cyclases manifest an apparent pH-sensitivity because of their activation by HCO_3^- ions[43]. Aside from these intracellular enzymes, H^+-sensing G protein-coupled receptors[44] (e.g. OGR1[45]), have been described in various cells, but these probe extracellular conditions, which is not appropriate for the purpose of auto-regulating the internal milieu.

To address these questions, we studied the effect of sustained extracellular acidity on pHi regulation using an *in vivo* model of infarction, which produces a diffuse pattern of myocardial lactic acidosis[46], and investigated the mechanism using a more tractable *in vitro* model of cultured myocytes adapted to acidic environments. We find that chronic exposure to extracellular acidity re-balances pHi control through changes in the expression of key pHi-regulator genes. This response is triggered by FAK1/Pyk2, an intracellular sensor of H^+ ions, which operates a feedback circuit that titrates the appropriate levels of transporters required to attain a favourable pHi over a range of pHe. We thus describe a secondary level of pHi oversight that is mandated at times when pHe is unstable or unreliable.

METHODS

Animal procedures. Animal experiments were approved by university ethical review boards and conform to the guidelines from Directive 2010/63/EU. For the cryo-infarct model, rats were anaesthetised by isoflurane (4% for induction, 2% for maintenance in O_2) delivered by intubation. Pre-/post-operative analgesia was provided (buprenorphine, meloxicam). Animals were euthanised by an approved procedure listed under Schedule 1 of the Animals (Scientific Procedures) Acts 1986: isoflurane overdose (adult rats), cervical dislocation (adult mice, neonatal rats), confirmed by the removal of the heart (cessation of circulation).

Cryo-induced myocardial infarction model. Procedures were carried out under licence PPL30-3322 in compliance with the requirements of the UK Home Office (ASPA1986 Amendments Regulations 2012), which includes an explicit cost-benefit analysis and independent ethical review. Male, 6-week old Sprague-Dawley rats were divided into cryo-injury or sham surgery groups. Animals were anesthetized by isoflurane in oxygen (4% for induction, 2% for maintenance), intubated for ventilation, and maintained on a heated pad with monitoring of temperature, pulse oxygenation and electrocardiogram (MouseMonitor S, Indus Instruments). Following a left thoracotomy and removal of the pericardium, the heart was stabilized by a loose stitch through the apex and myocardial infarction was induced by cryo-injury[46,47], via the placement of a 10 mm ø aluminium cylindrical probe cooled to 77 K onto the anterio-apical surface of the left ventricle for 15 seconds. The chest was closed in layers and the animal allowed to recover. In sham-operated rats, thoracotomy and cardiac exteriorization were performed, after which the chest was closed. All animals were provided with pre- and post-operative analgesia (buprenorphine and meloxicam) and lidocaine to prevent arrhythmia.

Oral bicarbonate supplementation. Procedures were carried out under licence PPL-P01A04016. Male, 7-week adult mice were given 400 mM bicarbonate water *ad lib* for 5 weeks. Control mice were housed separately and not given access to bicarbonate water.

^{13}C magnetic resonance. Hyperpolarized ^{13}C MRI and MRS were performed according to published methods, detailed in the Supplement.

pHLIP imaging. pH-low insertion peptide (pHLIP) is a construct that undergoes a pH-dependent conformational change, favouring membrane bilayer insertion at low pH. It has been shown that as extracellular pH falls below 6.5-7.0, pHLIP becomes anchored at the membrane[48]. When conjugated with a fluorescent dye, the construct can identify areas of acidity in tissues by fluorescent microscopy. pHLIP peptide Var3 was synthesized and purified by CS Bio Co. pHLIP peptide and Cy5.5-maleimide (Lumiprobe) were dissolved in DMSO, as described in the Supplement. Rats were tail-vein injected with a mixture of Var3 pHLIP fluorescently labelled with Cy5.5 (0.7 nmol/g in sterile PBS) and Hoechst-33342 (10mg/kg in sterile PBS) 5 h prior to tissue harvesting under license PPL PF8462746. Animals were killed humanely by an

approved Schedule 1 method and their hearts were excised, rinsed in PBS, blotted dry and mounted in trays of OCT before flash freezing in powdered dry ice. Long-axis sections were cut on a cryostat at 25µm thickness onto glass slides and stored at -80ºC. Images were taken on a Leica DM6000 microscope with a motorised stage, using Volocity 6.4.0 (Quorum Technologies) for automatic tiling. pHLIP (excitation 683 nm/emission 703 nm) and Hoechst (excitation 350 nm/emission 461 nm) were imaged sequentially. pHLIP and Hoechst images were individually background-subtracted and then normalized to the mean Hoechst signal within myocardial regions.

Isolation of adult ventricular myocytes. Adult rat myocytes were isolated from hearts using enzymatic digestion using a previously published method[49,50], and kept in primary culture for up to 10 h. In some experiments, animals were injected with Hoechst-33342 (10mg/kg in sterile PBS) 24 h prior to tissue harvesting under license PPL PF8462746 to label myocytes *in vivo* according to perfusion status.

Neonatal ventricular myocyte culture. Myocyte isolation and culture was performed as described previously[51]. Primary neonatal rat ventricular myocytes (NRVMs) were obtained from 1-2 day Sprague-Dawley rats euthanized by cervical dislocation. Cells were isolated by enzymatic digestion[52] and a 'pre-plating' step was introduced to reduce fibroblasts in the myocyte-containing supernatant. Cells were plated onto fibronectin-coated tissue culture dishes or Ibidi slides, and cultured in medium (referred to as M2) made of 80% DMEM medium containing 24 mM $NaHCO_3$ (D7777, Sigma/Merck) and 20% M199 medium with 26 mM $NaHCO_3$ (M4530, Sigma/Merck) and incubated in a 5% CO_2 atmosphere at 37°C. Medium was supplemented with 10% horse serum, 5% new born calf serum and penicillin/streptomycin mixture. Next day, medium was replaced by serum-free M2 supplemented with insulin-transferrin-selenium (ITS) and penicillin/streptomycin for 24 h. $NaHCO_3$ content was modified (2.2-24.4 mM) by iso-osmotic replacement with NaCl to achieve the desired pH[53].

Measuring intracellular pH with cSNARF. Myocytes were loaded with the acetoxymethyl ester of cSNARF1. When excited at a wavelength in the range 530-560 nm, cSNARF1 emits fluorescence that manifests a strongy pH-sensitive spectrum. By probing fluorescence at 580 nm and 640 nm, it is possible to record a ratio that is related to pH by the Grynkiewicz equation[53]. The cSNARF1 ratio can be calibrated

into units of pH by calibration experiments that use the H^+/K^+ ionophore nigericin, as described previously[10]. This calibration will be unique to a given set-up.

High-throughput fluorescence imaging. pHi of cultured NRVMs was imaged in black walled, flat-bottom 96 well plates (Ibidi). Media was aspirated from wells and replaced with Phenol-free media containing cSNARF1-AM (5 µg mL^{-1}, Molecular Probes) and Hoechst-33342 (10 µg mL^{-1}, Molecular Probes) for 15 min, and then replaced, twice, with dye-free medium. Images of fluorescence excited at 377 nm and collected at 447 nm (Hoechst), and of fluorescence excited at 531 nm and collected at 590 nm and 640 nm (cSNARF1), were acquired using Cytation 5 imaging plate reader (Biotek). All measurements were performed at 37°C. For media buffered with CO_2/HCO_3^-, measurements were performed in an atmosphere of 5% CO_2[53].

pH imaging under superfusion. Adult myocytes were imaged in superfusion chambers coated with poly-L-lysine to improve cell adhesion. Neonatal myocytes were imaged as monolayers grown in Ibidi chambers. Live-cell imaging was performed on a Zeiss LSM 700 confocal system. Myocytes were loaded for 10 minutes with 20 µM 5-(and-6)-carboxySNARF-1-AM ester (ThermoFisher Scientific). After loading, superfusates were delivered at 37°C, and recordings were made once the steady-state was attained (~10 min). cSNARF1 fluorescence was excited at 555 nm and measured at 580 and 640 nm. Hepes-buffered superfusates contained 135 mM NaCl, 4.5mM KCl, 1mM $MgCl_2$, 1mM $CaCl_2$, 11mM glucose, 20mM Hepes titrated to pH 7.4. CO_2/HCO_3^- buffered superfusates were modified to contain 125 mM NaCl and $NaHCO_3$ replaced Hepes, and the final solution was bubbled with 5% CO_2 (balanced with air). Low-chloride or chloride-free solutions were prepared by replacing Cl^- salts with gluconate equivalents, and correcting for Ca^{2+} complexation by raising [$CaCl_2$]. Ammonium- or acetate-containing solutions replaced NaCl with an equimolar amount of NH_4Cl or NaAcetate, respectively.

Antibodies and western blotting. Lysates were prepared from cardiac tissue or NRVMs by fine homogenisation or cell scraping in RIPA buffer with a phosphatase-protease inhibitor cocktail (Roche) on ice. Lysates were centrifuged and protein concentration was assessed by BCA assay. Samples were resolved on a 10% reducing SDS polyacrylamide gel and blotted on a PVDF membrane. Membranes were blocked for 1 h at RT in 3% bovine serum albumin for phospho-antibodies or 5%

low-fat milk for other antibodies in Tris-buffered saline and 0.1% Tween-20 (TBS-T). Primary antibodies were incubated overnight at 4ºC. Antibodies used were: total-Pyk2 (CST 3292S, 1:1000); phospho-Pyk2 Y402 (Abcam 4800, 1:1000); phospho-Pyk2 Y579/580 (Invitrogen 44-636G, 1:1000); AE2 (Novus NBP159858, 1:500); NHE1 (BD Biosciences 61175, 1:500). Membranes were washed with TBS-T and incubated with anti-rabbit/mouse HRP-conjugated secondary antibody (GE Healthcare Lifesciences). For loading controls, actin HRP-conjugated (Proteintech HRP60008, 1:20,000) and GAPDH HRP-conjugated (Proteintech HRP60004, 1:10,000) were used. Antibody-antigen complexes were visualised by Pierce™ enhanced chemiluminescent substrate with a Bio-Rad ChemiDoc™ Imaging System.

Statistics. Statistical testing of data involving myocytes was performed with hierarchical (nested) analysis[54]. Briefly, measurements on adult myocytes are reported as number of cells/number of hearts that yielded cells. Data were nested based on the heart they were obtained from. Measurements on neonatal myocytes are reported as number of wells/number of isolations (each typically from 10-12 pups). Data were nested based on isolation batch. Statistical testing considered the degree of interclass clustering. RNAseq data were analyzed by the DESeq2 package in R to identify significant hits with an adjusted P value smaller than 0.05 and log fold-change of at least 0.5.

RESULTS

Myocyte pHi undergoes a correction in acidic environments of infarcted hearts

As a consequence of their transport cycle, the ionic flux carried by sarcolemmal pHi-regulators responds acutely to changes in pHe. This results in a coupling between pHe and pHi at steady-state, which was measured in ventricular myocytes isolated from wild-type adult rats. Cells loaded with the pH-dye cSNARF1 were superfused with Tyrode solution over a range of pH, set by adjusting [HCO_3^-] at constant (5%) CO_2. At steady-state, typically attained within 30 minutes, the pHe–pHi relationship was linear, with a gradient of 0.25, meaning that pHi will drop below 7.0 when pHe is <6.9 (**Figure 1A**). Thus, despite having a pHi-regulatory apparatus capable of

generating H^+-fluxes as large as several mM/min, steady-state pHi is subservient to pHe. Consequently, chronic exposure to acidic environments, such as under-perfused niches in the developing or diseased myocardium, would drive pHi to low levels, unless corrected by an adaptive process that overcomes the thermodynamic pHe–pHi coupling.

To seek evidence for a re-setting of pHi control *in vivo* in response to chronic acidosis, adult rat hearts were subject to cryo-infarction to the apex of the left ventricle[47]. The technique produces a diffuse pattern of lactic acidosis across the myocardium and beyond the infarct region. The biological process underpinning this effect has been described previously by the co-authors[46]. Briefly, the source of lactate detected by magnetic resonance (MR) imaging is primarily the release from infiltrating macrophages, and some production also taking place in the blood. Lactate is a highly mobile anion, which leads to a diffuse appearance of its MR signal across the heart. To confirm this spatial pattern in the present cohort of animals, lactate and bicarbonate were measured by hyperpolarised ^{13}C MR imaging three days after cryo-infarction. The injury resulted in a diffuse build-up of lactate and a depletion of bicarbonate across a large part of the myocardium (**Figure 1B**). This pattern of lactate and bicarbonate is expected to result in diffusely distributed extracellular acidosis, which could the trigger pH-driven adaptive responses over a larger part of the heart. To test that cryo-injury results in a diffuse pattern of chronic extracellular acidosis beyond the injury site, rats were administered a mixture of the acid-detecting peptide pHLIP and the nuclear stain Hoechst, delivered by tail vein injection at 2 weeks post-surgery. After allowing 5 h for systemic distribution, hearts were harvested for sectioning and imaging. Fluorescence from Cy5.5-conjugated pHLIP was normalized to the tissue-averaged Hoechst signal and presented in **Figure 1C**, and quantified in **Figure S1**. Compared to sham-operated animals, there was a diffuse distribution of pHLIP fluorescence, indicating that large areas of the myocardium were acidotic at 2 weeks after surgery. Any form of adaptation to this chronic extracellular acidity would be expected to take place over a large area of the myocardium. Adaptive responses to chronic acidosis were measured at a later time point, to ensure sufficient time for their implementation. In terms of indices such as ejection fraction, the remodelling process evoked by cryo-injury can be significantly resolved from sham controls by 5 weeks following

surgery[47,55]. For this reason, the 5-week time point was selected to seek evidence for an adaptation of pHi control to a period of sustained acidosis.

Myocardial pHi was measured *in vivo* by hyperpolarised [^{13}C]-pyruvate MRI from the ratio of $^{13}CO_2$ to $H^{13}CO_3^-$ peaks in rats five weeks after cryo-injury or sham-surgery. Despite the low pHe reported by pHLIP, *in vivo* pHi measured by hyperpolarised ^{13}C MR spectroscopy was not significantly different to that determined in sham-operated hearts (**Figure 1D**). To test if this convergence in pHi reflects an adaptive resetting of pHi regulation in hearts recovering from cryo-injury, enzymically isolated myocytes were imaged fluorescently for pHi under superfusion with CO_2/HCO_3^- buffer at pHe 7.4. In the case of hearts recovering from cryo-infarction, resting pHi was significantly higher in isolated myocytes under superfusion compared to cells in the beating heart (**Figure 1D**). In contrast, the pHi in sham-operated hearts was no different between *in vivo* and *ex vivo* measurements. Taken together, these data indicate that myocytes in cryo-infarcted hearts had adapted to their acidic environment by correcting pHi, which becomes evident as a pHi overshoot upon superfusion at physiological pHe (**Figure 1E**).

The most profound adaptation of pHi control to acidic environments *in vivo* is expected in areas that are least perfused. Myocytes derived from such under-perfused niches can be identified from nuclear Hoechst staining, after injecting the dye for systemic distribution prior to cell isolation. Thus, 5 weeks following cryo-injury, rats were injected intravenously with a bolus of Hoechst, followed by enzymic isolation of cells 24 hours later. Isolated myocytes emitting the strongest Hoechst signal would be derived from well-perfused areas. To quantify nuclear Hoechst signal, fluorescence collected within the cell outline was analysed for bimodality to determine a threshold that separates the low background in cytoplasm from the nuclear signal, if stained (**Figure 1F**). Signal summated above the threshold was normalized to total signal in the cell; this provided an index that quantifies the degree of nuclear staining, ranging from zero in myocytes derived from the least perfused regions of myocardium, to a high signal in cells from the best perfused regions (**Figure 1G**). There was a significant correlation between perfusion (as determined by Hoechst signal) and pHi, measured in the presence or absence of CO_2/HCO_3^- buffer. Cells from the least perfused niches had undergone the most profound remodelling of pHi control. Thus, an adaptive process takes place in myocytes *in situ* in response to inadequate perfusion. The

outcome is a re-establishment of pHi homeostasis by overcoming the thermodynamic challenge arising from pHe-pHi coupling.

Adaptation to acidity involves a re-balancing of myocyte pHi control

The re-setting of pHi in the infarcted heart must involve a rebalancing of fluxes carried by sarcolemmal acid-base transporters. To characterise this, H^+-equivalent transport was measured in myocytes isolated from cryo-infarcted or sham-operated hearts at five weeks after surgery to allow adaptive processes to take place. In order to calculate flux, intrinsic pH buffering was measured using a stepwise ammonium removal protocol[10] (**Figure 2A**). Buffering was no different between sham and cryo-infarcted heart, and therefore a pooled buffering line was used for flux analyses. NHE1 activity was measured by the ammonium prepulse method in the absence of CO_2/HCO_3^- (**Figure 2B**) and NBC activity was determined in the presence of CO_2/HCO_3^- and 30 µM dimethyl amiloride (**Figure 2C**). CBE activity was determined by acetate prepulse, with an intermediate step in chloride-free solution to allow CO_2/HCO_3^- buffer equilibration prior to acid-loading[11] (**Figure 2D**). Hierarchical statistical analyses showed that myocytes from cryo-infarcted hearts produced significantly smaller acid-loading by CBE but higher acid-extrusion by NHE1, whereas NBC activity was unchanged. This increase in the ratio of NHE1-to-CBE activity is a means of offsetting set-point pHi.

Lysates prepared from cryo-damaged hearts had higher NHE1 immunoreactivity relative to sham controls as well as un-operated age-matched hearts, indicating that the increase in NHE1-carried flux involves, at least in part, a change in expression (**Figure 2E**). This effect may relate to a myriad of changes associated with infarction, so to test if NHE1 expression was generally responsive to pHe, a series of experiments were performed on animals with raised systemic buffering, which produces a more stable pHe environment for myocytes in the heart. To attain this, mice were given bicarbonate in drinking water *ad lib* for 5 weeks[56]. At the end of the protocol, cardiac lysates were prepared for immunoblotting. Higher systemic buffering reduced NHE1 immunoreactivity relative to control mice, consistent with a more stable pHe (**Figure 2F**). Taken together with observations on hearts

recovering from infarction, these findings indicate that the pHi-regulatory apparatus responds to sustained changes in ambient pHe in both directions.

Adaptation of pHi control to acidic environments involves changes in Slc4a2, Slc9a1, and Slc4a7 expression

Cultured myocytes are a tractable model for mechanistic studies into the process of acid adaptation. To determine the suitability of this system for such investigations, it was first necessary to demonstrate that the *in vivo* actions of chronically low pHe on pHi control could be replicated *in vitro*. Experiments were performed on cultured neonatal rat ventricular myocytes (NRVMs). NRVMs were incubated at pHe 6.4 (acid-stimulus) or 7.4 (control) for 48 h, and then dually loaded with cSNARF1 (to measure pHi) and Hoechst (to identify nuclei) for imaging. Fluorescence images were acquired on a high-throughput imaging platform and an offline analysis pipeline generated the statistical distribution of pHi (**Figure 3A**). The pHi-regulatory apparatus of myocytes was interrogated in terms of its acute pHe-sensitivity (i.e. pHe-pHi coupling), determined after allowing ~30 min for equilibration with media over a range of pHe (6.4-7.4), attained by varying [HCO_3^-] at constant (5%) CO_2. Parallel experiments were performed in the presence of 30 µM cariporide added 4 h prior to imaging to block the contribution from NHE1, and in low-chloride media replaced 4 h before imaging to hinder acid-loading flux carried by CBE. To characterise the effect of long-term acidosis on pHi control, measurements were performed on myocytes that had been incubated for 48 h at pH 6.4 (acid-adapted) or 7.4 as its control (**Figure 3B**). In general, pHe-pHi curves shifted downwards with cariporide and upwards in low-chloride media, confirming that steady-state pHi is set by the balance between acid-extruding NHE1 and acid-loading CBE. After 48 h in acidic media, these pHe-pHi curves shifted in the alkaline direction, indicating that pHi control had adapted to the acidic environment. Notably, the pHe-pHi relationship became more curved in acid-adapted myocytes, which ensures a more alkaline pHi over a wide range of pHe. For example, myocytes kept at pHe 7.4 were able to maintain pHi>7.0 over acute pHe-disturbances down to pHe 6.7 only, whereas acid-adapted myocytes could do so over a wider pHe range, down to pHe 6.5. This

adaptation confers a clear advantage, as it enables cardiac functions to operate in their optimal pHi range, even when the cellular environment sustains chronic acidity.

Additional pHe-pHi curves were measured for NRVMs adapted to a range of pHe (**Figure 3C/D**). In general, adaptation to acidic media tended to increase the steepness and curvature of the pHe-pHi curve. The events that result in these outcomes can be summarised in terms of an iterative process, shown in **Figure 3D**. Initially, exposure to an acidic environment thermodynamically drives pHi to a lower level; over time, cells respond to the sustained acidosis through an adaptive process that offsets, albeit partially, the thermodynamic challenge. **Figure 3E** illustrates this process using frequency distributions of pHi measured under control conditions, in response to an acute displacement of pHe to 6.9, and following 48-h adaptation to pH 6.9.

The mechanism underpinning the adaptation to acidity was interrogated functionally in terms of acid-extrusion and acid-loading fluxes, measured by ammonium and acetate prepulse, respectively. To make comparisons at matching conditions, experiments used CO_2/HCO_3^- buffered superfusates at pH 7.4. Acid-adapted NRVMs presented with higher acid-extrusion (**Figure 3F**) and lower acid-loading fluxes, relative to time-matched controls incubated at pH 7.4 (**Figure 3G**). This re-balancing explains how the setpoint pHi increases in acid-adapted myocytes. Since these measurements were performed in superfusates at pH 7.4 within 1 h of withdrawing the acid-stimulus, the effect of acid-adaptation must involve a sustained change in transporter activity, such as a shift in the expression of genes coding for acid-base transporters. Analysis of RNAseq transcriptomics of NRVMs treated for 48 h in pHe ranging from 6.4 to 7.4 identified three pHe-responsive genes implicated in pHi control: *Slc4a2* (coding for AE2), *Slc9a1* (coding for NHE1), and *Slc4a7* (coding for NBCn1). As part of adaptation to low pHe, expression of acid-loading *Slc4a2* decreased whereas expression of acid-extruding *Slc9a1* and *Slc4a7* increased (**Figure 3H**). The response of *Slc9a1* and *Slc4a2* is consistent with data for NHE1 and CBE fluxes measured in the cryo-infarct model, and was confirmed at protein level in NRVMs by western blot, showing upregulation of NHE1 protein and downregulation of AE2 protein (**Figure 3I**; quantified in **Figure S2**).

Acid-adaptation of pHi control is instigated by FAK family intracellular H^+-sensors

To investigate the time course of the acid-adaptation response, experiments were performed on NRVMs exposed to acidic media (pH 6.4) for a shorter, 4-h period. This protocol was not sufficient to fully develop the acid-adaptation response to 48-h acidity (**Figure 4A**), which is consistent with acid-adaptation being a slow-onset process, such as involving a change in gene expression. The mechanism of acid-adaptation was investigated further in myocytes subjected to various interventions during the 48 h incubation period. The underlying sensing mechanism may gauge pH directly from the level of H^+ ions, or indirectly from HCO_3^- ions. A precedent for the latter are CO_2/HCO_3^- sensitive soluble adenylyl cyclases residing intracellularly and receptor tyrosine phosphatase γ (RTPγ) which presents an exofacial HCO_3^- sensor. To distinguish these alternative sensor ligands, acid-adaptation was performed in the absence of CO_2/HCO_3^-, replacing this buffer with an equimolar mixture of Hepes and Mes (in 0% CO_2). At the end of the experiment, the pHe-pHi relationships were mapped in the presence of CO_2/HCO_3^- buffer, and compared with controls that had been acid-adapted in CO_2/HCO_3^- throughout. In the nominal absence of CO_2/HCO_3^- during incubation, a 48-h period in acidity was still able to shift the pHe-pHi relationship upwards, indicating that the sensor is triggered by H^+ ions and not components of CO_2/HCO_3^- (**Figure 4B**).

The change in the expression of genes responsible for pHi-regulation may be triggered by an exofacial sensor, detecting low pHe, or an intracellular sensor that probes the knock-on effect on pHi. Extracellular facing receptors have been widely studied in various tissues, and include receptors for H^+ ions, such as the G protein-coupled receptor OGR1. Strategically, however, an intracellular sensor would be best placed to gauge the outcome of a cellular adaptation to pHe. To distinguish these alternative locations, NRVMs were incubated in low-chloride media, a manoeuvre that raises pHi at constant pHe because of cytoplasmic loading with HCO_3^- ions. It is therefore possible to expose NRVMs to acidic media for 48 h, without evoking the full extent of the pHi decrease. The protocols for this experiment are shown in **Figure 4C**. Cells were adapted to pH 6.9 or 7.4 in either low- or normal-chloride media for 48 h, followed by measurements at matching conditions, all in CO_2/HCO_3^- buffer. The controls for these experiments were cells that had been incubated in pH 7.4 in normal-

chloride media, and then probed at 6.9 or 7.4 in either low- or normal-chloride media. In normal-chloride media, incubation at low pH evoked the expected adaptive response (shown by green arrow). However, this effect was absent in parallel experiments performed under low-chloride conditions. Together, these findings implicate an intracellular H^+ sensor, which becomes engaged when pHi falls, but not when cells are HCO_3^--overloaded in low-chloride media (**Figure 4C**). To verify this observation at the level of gene expression, qPCR measurements of *Slc9a1* were performed in NRVMs cultured at 7.4 or at 6.9 in normal-chloride media or at 7.4, 6.9 or 6.4 in low-chloride formulations (**Figure 4D**). The gene coding for NHE1 (*Slc9a1*) was upregulated only under conditions that allowed pHi to fall, i.e. acidic media of normal chloride, but not when pHi was raised in low-chloride formulations.

There is a myriad of candidates for the intracellular H^+ sensor, which may take the form of a discrete receptor, or be devolved among many proteins collectively manifesting pHi sensitivity. A notable pH-dependent process that feeds into gene expression is histone acetylation. To test if adaptation to low pHe is dependent on a change in acetylation, a broad-spectrum histone deacetylase inhibitor, SAHA (10 µM), was applied during the 48-h incubation period at pH 6.4 or 7.4. Acetylases are generally inhibited at low pH, but this effect would be cancelled-out in the presence of SAHA. However, SAHA did not affect the acid-adaptation response (**Figure 5A**).

A plausible mechanism for regulating SLC-type genes may involve kinases. Among published transcriptomics datasets for the effect of twenty-six FDA-approved kinase inhibitors on gene expression in human cardiac cells[57], several drugs were found to affect the expression of at least one of the genes involved in acid-adaptation (*SLC9A1, SLC4A2, SLC4A7;* **Table S1**). Thus, kinase-operated pathways are candidates for transducing a sustained acid signal onto a change in pHi regulation. Culture media for NRVMs are, per standard protocol, supplemented with insulin-transferrin-selenium (ITS), and the operation of its downstream signalling pathway may endow pH sensitivity. However, removing ITS in the 48-h acid-incubation period had no effect on acid-adaptation outcomes (**Figure 5B**).

Kinases that have been ascribed a *bona fide* pH-sensing role include two members of the FAK family, FAK1[40] and FAK2 (Pyk2)[41,42]. These non-receptor tyrosine kinase[58-60] have a histidine-rich FERM domain believed to mediate the effect

of pHi on auto-phosphorylation. The FAK1/Pyk2 inhibitor PF-431396 (10 µM), when included for the duration of acid-treatment, ablated the acid-adaptation response of pHi control. In particular, the ensuing pHe-pHi relationship lacked the characteristic curvature normally attained with acid-adaptation (**Figure 5C**). This effect was not observed when PF-431396 was added for the final 4 h of acid-treatment and during imaging (**Figure 5D**), indicating that the inhibitor must target an early step in the acid-adaptation response to produce its effect. Src kinases are part of the FAK signalling pathway, and have been implicated as the enzymes responsible for phosphorylating FAK1 and Pyk2 following their auto-phosphorylation. However, the Abl/Src kinase inhibitor Dasatinib (100 nM) did not phenocopy the effect of PF-431396, suggesting that H^+ ions act at the level of FAK autophosphorylation (**Figure 5E**).

Of the two FAK family kinases, an earlier series of renal studies[41,42] had implicated Pyk2 in a feedback loop linking intracellular acidification with higher acid-extrusion activity. This process resembles the response in myocytes described herein. The renal mechanism was proposed to involve the release of endothelin-1 (ET1), but acid-adaptation in myocytes was unaffected by the presence of the ET1 receptor antagonist bosentan (10 µM), arguing against the involvement of ET1 (**Figure 5F**).

The involvement of FAK1/Pyk2 in the link between chronic acidosis and NHE1 expression was tested pharmacologically. Neonatal myocytes were incubated at either pH 6.4 or 7.4 for 48 h in the presence or absence of PF-431396. Cells treated with PF-431396 had significantly reduced NHE1 expression, indicating that the inhibition of FAK-family kinases causes the pHi-regulatory apparatus to favour a more acidic set-point pHi (**Figure 5G**).

To seek evidence that cardiomyocyte FAK1 and Pyk2 proteins respond post-translationally to an acidic stimulus, western blotting was performed on NRVMs exposed to acidic media (pH 6.4) for 10 min, 30 min or 48 h, with appropriate time-matched controls (pH 7.4). An acid-evoked decrease in Y579/580 phosphorylation was detectable after 10 min of treatment, indicating a rapid-onset effect compatible with a trigger of acid-adaptation (**Figure 6A**). The same treatment protocols produced a more modest decrease in FAK1 phosphorylation at Y397 (**Figure 6B**). In summary, exposure to acidic conditions triggers, within minutes, a response in the FAK family proteins Pyk2 and FAK1, the putative intracellular H^+ sensors. Inhibiting FAK proteins

pharmacologically ablates the acid-adaptation of pHi control, and decreases expression of NHE1.

DISCUSSION

The urgency of maintaining a favourable pHi is demonstrated by the observation that cardiac physiology is highly pHi-sensitive[1-9] and that the sarcolemma can generate H^+-equivalent fluxes as large as tens of mM/min to correct pHi disturbances, notably the largest of all ionic fluxes recorded in cardiac cells[10-14]. The regulatory prowess of acid-base transporters has often led to the assumption that pHi is held firmly constant, unless directed to change by neurohormonal factors. However, a major vulnerability in the system relates to its sensitivity to *extracellular* pH, a thermodynamic consequence of the transport cycle[24,27,28]. Whereas pHi-sensitivity is obligatory for a homeostatic regulator of the internal milieu, the dependence on pHe should be considered a regulatory flaw, because it inadvertently transfers the chemical vulnerability of the extracellular milieu onto the myocyte. This thermodynamic coupling would compromise pHi control – and hence cardiac function – unless a corrective factor is implemented. This issue is particularly relevant to under-perfused niches emerging in disease states, such as the infarcted heart[30,61], or developmentally when vascular perfusion is undergoing maturation or unstable[62-64]. Beyond the heart, a similar concern can apply to cerebral ischemia, because neuronal function is also highly pH-sensitive[65,66]. It has therefore been speculated that a secondary level of pHi control is necessary to correct for the coupling between pHe and pHi.

Herein, we describe a secondary layer of pHi homeostasis which re-balances the expression of acid-base transporters, notably *Slc4a2* and *Slc9a1*, until their fluxes return steady-state pHi towards 7.1-7.2. This correction was observed *in vivo* in hearts following a period of recovery after cryo-infarction, a surgical intervention that produces a diffuse pattern of extracellular lactic acidosis, as well as in animals with orally supplemented systemic buffering, which helps to maintain interstitial alkalinity near contracting myocytes. Myocytes adapt to the extracellular acidosis of the infarcted heart by increasing acid-extrusion capacity by NHE1 and decreasing acid-

loading by CBE. This response can restore a near-normal pHi in the beating heart, despite the persistence of the underlying extracellular acidosis. The adaptive correction was revealed as an overshoot in pHi after cells had been enzymically liberated and superfused at physiological pHe. Myocytes derived from the most under-perfused niches, determined by *in vivo* Hoechst staining, had the greatest degree of pHi remodelling. Consistent with a demand for more acid-extrusion to raise pHi, NHE1 expression increased in the recovery period after cryo-infarction. In contrast, a reduction in demand for acid-extrusion in animals on an oral bicarbonate regime resulted in NHE1 downregulation, indicating that NHE1 expression is titrated on a needs basis. In these studies, NHE1 immunoreactivity was used as a readout of pHi control because anti-NHE1 antibodies are optimised for adequate densitometric quantification on western blot.

The response to acid-adaptation could be replicated *in vitro* using neonatal myocytes, which enabled further mechanistic studies using a high-throughput pipeline of analysis. Transcriptomics identified three members of the 'intracellular pH regulation' ontology that respond to pHe: *Slc4a2*, *Slc9a1*, or *Slc4a7*. This result was confirmed at protein level for NHE1 and AE2 and functionally, from sarcolemmal flux measurements. The ligand for the 'acid sensor' that triggers this response was determined to be H^+ ions, rather than other acid-base proxies such as CO_2/HCO_3^-, the trigger for soluble adenylyl cyclase or receptor tyrosine phosphatase gamma (RTPγ). The location of this H^+ sensor was intracellular, rather than exofacial, which is desirable for a system designed to oversee pHi. The onset of the acid-adaptation response was slow, taking many hours, and its consequences on pHi control persisted after withdrawing the acid-treatment, at least in the time frame of measurements.

Although histone acetylation is known to be pH-sensitive, through the catalytic responses of acetyl-transferase and deacetylase enzymes[39], pharmacological inhibition of HDACs had no effect on the acid-adaptation response. Transcriptomics profiling identified various kinase that affect the expression of *Slc4a2*, *Slc9a1*, or *Slc4a7*, and taken together with known candidates for pH sensors, highlighted FAK family non-receptor tyrosine kinases (FAK1/Pyk2)[41,42] as possible transducers of acid-adaption. Indeed, acidic conditions evoked a change in FAK1 and Pyk2 phosphorylation and FAK inhibition ablated the acid-adaptation response of pHi control by decreasing the expression of NHE1. Drugs acting upstream to FAK had no

effect on acid-adaptation outcomes, indicating FAK proteins as the entry point for H^+ signals. Although protonation is an almost universal post-translational modification, only a small number of proteins have met the criteria for *bona fide* acid-sensors. These sensors include FAK-family proteins. However, additional pH-sensing components contributing towards the process of acid-adaptation cannot be excluded, as pharmacological FAK inhibition does not completely ablate the response measured in terms of pHi.

In summary, we have characterised how myocytes adapt their pHi-regulatory apparatus to acidic conditions, and thereby overcome the thermodynamic coupling between pHe and pHi, which would otherwise transfer the vulnerability of the external milieu onto unwarranted changes in pHi. The mechanism, operated by intracellular H^+ sensors, also explains how the gene expression apparatus is instructed to titrate the correct level of acid-loaders and acid-extruders in order to attain physiological pHi. The operation of this feedback system also explains how a cardiomyocyte determines what is deemed to be normal pHi. In future studies, it would be prudent to investigate the role of these pH-sensing mechanisms in other tissues, notably the brain, which is also susceptible to ischemia.

FUNDING

British Heart Foundation Programme Grant RG/15/9/31534 (to PS), and RG/11/9/28921 (to DJT). This work was partially supported by the National Institutes of Health grant NIH RO1 GM073857 to OAA and YKR.

AUTHOR CONTRIBUTION STATEMENT

AW, MAR, MKC, MR, JJM, AJL, VB, SM, AAL and CC performed the research. AM, DJT, OAA and YKR provided research materials. PS supervised the work. PS wrote the manuscript, and all authors contributed to the final draft.

ACKNOWLEDGMENTS

We thank Chela Alonso for isolating cardiac myocytes.

DISCLOSURES

Competing Interest Statement: OAA and YKR are founders of pHLIP, Inc. They have shares in the company, but the company did not fund any part of the work reported in this paper.

DATA AVAILABILITY STATEMENT

The data underlying this article are available in the article and in its online supplementary material. The data underlying this article will be shared on reasonable request to the corresponding author.

REFERENCES

1. Garciarena CD, Youm JB, Swietach P, Vaughan-Jones RD. H(+)-activated Na(+) influx in the ventricular myocyte couples Ca(2)(+)-signalling to intracellular pH. *J Mol Cell Cardiol* 2013;**61**:51-59.
2. Vaughan-Jones RD, Spitzer KW, Swietach P. Intracellular pH regulation in heart. *J Mol Cell Cardiol* 2009;**46**:318-331.
3. Fabiato A, Fabiato F. Effects of pH on the myofilaments and the sarcoplasmic reticulum of skinned cells from cardiace and skeletal muscles. *J Physiol* 1978;**276**:233-255.
4. Bountra C, Vaughan-Jones RD. Effect of intracellular and extracellular pH on contraction in isolated, mammalian cardiac muscle. *J Physiol* 1989;**418**:163-187.
5. Orchard CH, Kentish JC. Effects of changes of pH on the contractile function of cardiac muscle. *Am J Physiol* 1990;**258**:C967-981.
6. Harrison SM, Frampton JE, McCall E, Boyett MR, Orchard CH. Contraction and intracellular Ca2+, Na+, and H+ during acidosis in rat ventricular myocytes. *Am J Physiol* 1992;**262**:C348-357.
7. Allen DG, Orchard CH. The effects of changes of pH on intracellular calcium transients in mammalian cardiac muscle. *J Physiol* 1983;**335**:555-567.
8. Choi HS, Trafford AW, Orchard CH, Eisner DA. The effect of acidosis on systolic Ca2+ and sarcoplasmic reticulum calcium content in isolated rat ventricular myocytes. *J Physiol* 2000;**529 Pt 3**:661-668.
9. Orchard CH, Cingolani HE. Acidosis and arrhythmias in cardiac muscle. *Cardiovasc Res* 1994;**28**:1312-1319.
10. Leem CH, Lagadic-Gossmann D, Vaughan-Jones RD. Characterization of intracellular pH regulation in the guinea-pig ventricular myocyte. *J Physiol* 1999;**517 (Pt 1)**:159-180.
11. Sun B, Leem CH, Vaughan-Jones RD. Novel chloride-dependent acid loader in the guinea-pig ventricular myocyte: part of a dual acid-loading mechanism. *J Physiol* 1996;**495 (Pt 1)**:65-82.
12. Poole RC, Halestrap AP, Price SJ, Levi AJ. The kinetics of transport of lactate and pyruvate into isolated cardiac myocytes from guinea pig. Kinetic evidence for the presence of a carrier distinct from that in erythrocytes and hepatocytes. *Biochem J* 1989;**264**:409-418.

13. Lagadic-Gossmann D, Buckler KJ, Vaughan-Jones RD. Role of bicarbonate in pH recovery from intracellular acidosis in the guinea-pig ventricular myocyte. *J Physiol* 1992;**458**:361-384.
14. Xu P, Spitzer KW. Na-independent Cl(-)-HCO3- exchange mediates recovery of pHi from alkalosis in guinea pig ventricular myocytes. *Am J Physiol* 1994;**267**:H85-91.
15. Orlowski J, Grinstein S. Diversity of the mammalian sodium/proton exchanger SLC9 gene family. *Pflugers Arch* 2004;**447**:549-565.
16. Sardet C, Franchi A, Pouyssegur J. Molecular cloning, primary structure, and expression of the human growth factor-activatable Na+/H+ antiporter. *Cell* 1989;**56**:271-280.
17. Choi I, Romero MF, Khandoudi N, Bril A, Boron WF. Cloning and characterization of a human electrogenic Na+-HCO-3 cotransporter isoform (hhNBC). *Am J Physiol* 1999;**276**:C576-584.
18. Romero MF, Fulton CM, Boron WF. The SLC4 family of HCO 3 - transporters. *Pflugers Arch* 2004;**447**:495-509.
19. Yamamoto T, Shirayama T, Sakatani T, Takahashi T, Tanaka H, Takamatsu T, Spitzer KW, Matsubara H. Enhanced activity of ventricular Na+-HCO3- cotransport in pressure overload hypertrophy. *Am J Physiol Heart Circ Physiol* 2007;**293**:H1254-1264.
20. Virkki LV, Wilson DA, Vaughan-Jones RD, Boron WF. Functional characterization of human NBC4 as an electrogenic Na+-HCO cotransporter (NBCe2). *Am J Physiol Cell Physiol* 2002;**282**:C1278-1289.
21. Grichtchenko, II, Choi I, Zhong X, Bray-Ward P, Russell JM, Boron WF. Cloning, characterization, and chromosomal mapping of a human electroneutral Na(+)-driven Cl-HCO3 exchanger. *J Biol Chem* 2001;**276**:8358-8363.
22. Alper SL. Molecular physiology of SLC4 anion exchangers. *Exp Physiol* 2006;**91**:153-161.
23. Richards SM, Jaconi ME, Vassort G, Puceat M. A spliced variant of AE1 gene encodes a truncated form of Band 3 in heart: the predominant anion exchanger in ventricular myocytes. *J Cell Sci* 1999;**112 (Pt 10)**:1519-1528.
24. Niederer SA, Swietach P, Wilson DA, Smith NP, Vaughan-Jones RD. Measuring and modeling chloride-hydroxyl exchange in the Guinea-pig ventricular myocyte. *Biophys J* 2008;**94**:2385-2403.
25. Alvarez BV, Kieller DM, Quon AL, Markovich D, Casey JR. Slc26a6: a cardiac chloride-hydroxyl exchanger and predominant chloride-bicarbonate exchanger of the mouse heart. *J Physiol* 2004;**561**:721-734.
26. Shcheynikov N, Wang Y, Park M, Ko SB, Dorwart M, Naruse S, Thomas PJ, Muallem S. Coupling modes and stoichiometry of Cl-/HCO3- exchange by slc26a3 and slc26a6. *J Gen Physiol* 2006;**127**:511-524.
27. Vaughan-Jones RD, Wu ML. Extracellular H+ inactivation of Na(+)-H+ exchange in the sheep cardiac Purkinje fibre. *J Physiol* 1990;**428**:441-466.
28. Jean T, Frelin C, Vigne P, Barbry P, Lazdunski M. Biochemical properties of the Na+/H+ exchange system in rat brain synaptosomes. Interdependence of internal and external pH control of the exchange activity. *J Biol Chem* 1985;**260**:9678-9684.
29. Steenbergen C, Deleeuw G, Rich T, Williamson JR. Effects of acidosis and ischemia on contractility and intracellular pH of rat heart. *Circ Res* 1977;**41**:849-858.
30. Garlick PB, Radda GK, Seeley PJ. Studies of acidosis in the ischaemic heart by phosphorus nuclear magnetic resonance. *Biochem J* 1979;**184**:547-554.
31. Yan GX, Kleber AG. Changes in extracellular and intracellular pH in ischemic rabbit papillary muscle. *Circ Res* 1992;**71**:460-470.
32. Sardet C, Counillon L, Franchi A, Pouyssegur J. Growth factors induce phosphorylation of the Na+/H+ antiporter, glycoprotein of 110 kD. *Science* 1990;**247**:723-726.
33. Moolenaar WH, Tsien RY, van der Saag PT, de Laat SW. Na+/H+ exchange and cytoplasmic pH in the action of growth factors in human fibroblasts. *Nature* 1983;**304**:645-648.

34. Lagadic-Gossmann D, Vaughan-Jones RD. Coupling of dual acid extrusion in the guinea-pig isolated ventricular myocyte to alpha 1- and beta-adrenoceptors. *J Physiol* 1993;**464**:49-73.
35. Puceat M, Clement-Chomienne O, Terzic A, Vassort G. Alpha 1-adrenoceptor and purinoceptor agonists modulate Na-H antiport in single cardiac cells. *Am J Physiol* 1993;**264**:H310-319.
36. Matsui H, Barry WH, Livsey C, Spitzer KW. Angiotensin II stimulates sodium-hydrogen exchange in adult rabbit ventricular myocytes. *Cardiovasc Res* 1995;**29**:215-221.
37. Gunasegaram S, Haworth RS, Hearse DJ, Avkiran M. Regulation of sarcolemmal Na(+)/H(+) exchanger activity by angiotensin II in adult rat ventricular myocytes: opposing actions via AT(1) versus AT(2) receptors. *Circ Res* 1999;**85**:919-930.
38. Richards MA, Simon JN, Ma R, Loonat AA, Crabtree MJ, Paterson DJ, Fahlman RP, Casadei B, Fliegel L, Swietach P. Nitric oxide modulates cardiomyocyte pH control through a biphasic effect on sodium/hydrogen exchanger-1. *Cardiovasc Res* 2020;**116**:1958-1971.
39. McBrian MA, Behbahan IS, Ferrari R, Su T, Huang TW, Li K, Hong CS, Christofk HR, Vogelauer M, Seligson DB, Kurdistani SK. Histone acetylation regulates intracellular pH. *Mol Cell* 2013;**49**:310-321.
40. Choi CH, Webb BA, Chimenti MS, Jacobson MP, Barber DL. pH sensing by FAK-His58 regulates focal adhesion remodeling. *J Cell Biol* 2013;**202**:849-859.
41. Preisig PA. The acid-activated signaling pathway: starting with Pyk2 and ending with increased NHE3 activity. *Kidney Int* 2007;**72**:1324-1329.
42. Li S, Sato S, Yang X, Preisig PA, Alpern RJ. Pyk2 activation is integral to acid stimulation of sodium/hydrogen exchanger 3. *J Clin Invest* 2004;**114**:1782-1789.
43. Chen Y, Cann MJ, Litvin TN, Iourgenko V, Sinclair ML, Levin LR, Buck J. Soluble adenylyl cyclase as an evolutionarily conserved bicarbonate sensor. *Science* 2000;**289**:625-628.
44. Tomura H, Mogi C, Sato K, Okajima F. Proton-sensing and lysolipid-sensitive G-protein-coupled receptors: a novel type of multi-functional receptors. *Cell Signal* 2005;**17**:1466-1476.
45. Ludwig MG, Vanek M, Guerini D, Gasser JA, Jones CE, Junker U, Hofstetter H, Wolf RM, Seuwen K. Proton-sensing G-protein-coupled receptors. *Nature* 2003;**425**:93-98.
46. Lewis AJM, Miller JJ, Lau AZ, Curtis MK, Rider OJ, Choudhury RP, Neubauer S, Cunningham CH, Carr CA, Tyler DJ. Noninvasive Immunometabolic Cardiac Inflammation Imaging Using Hyperpolarized Magnetic Resonance. *Circ Res* 2018;**122**:1084-1093.
47. Ciulla MM, Paliotti R, Ferrero S, Braidotti P, Esposito A, Gianelli U, Busca G, Cioffi U, Bulfamante G, Magrini F. Left ventricular remodeling after experimental myocardial cryoinjury in rats. *J Surg Res* 2004;**116**:91-97.
48. Sosunov EA, Anyukhovsky EP, Sosunov AA, Moshnikova A, Wijesinghe D, Engelman DM, Reshetnyak YK, Andreev OA. pH (low) insertion peptide (pHLIP) targets ischemic myocardium. *Proc Natl Acad Sci U S A* 2013;**110**:82-86.
49. Ford KL, Moorhouse EL, Bortolozzi M, Richards MA, Swietach P, Vaughan-Jones RD. Regional acidosis locally inhibits but remotely stimulates Ca2+ waves in ventricular myocytes. *Cardiovasc Res* 2017;**113**:984-995.
50. Chung YJ, Luo A, Park KC, Loonat AA, Lakhal-Littleton S, Robbins PA, Swietach P. Iron-deficiency anemia reduces cardiac contraction by downregulating RyR2 channels and suppressing SERCA pump activity. *JCI Insight* 2019;**4**.
51. Loonat AA, Curtis MK, Richards MA, Nunez-Alonso G, Michl J, Swietach P. A high-throughput ratiometric method for imaging hypertrophic growth in cultured primary cardiac myocytes. *J Mol Cell Cardiol* 2019;**130**:184-196.
52. Zoccarato A, Surdo NC, Aronsen JM, Fields LA, Mancuso L, Dodoni G, Stangherlin A, Livie C, Jiang H, Sin YY, Gesellchen F, Terrin A, Baillie GS, Nicklin SA, Graham D, Szabo-Fresnais N, Krall J, Vandeput F, Movsesian M, Furlan L, Corsetti V, Hamilton

G, Lefkimmiatis K, Sjaastad I, Zaccolo M. Cardiac Hypertrophy Is Inhibited by a Local Pool of cAMP Regulated by Phosphodiesterase 2. *Circ Res* 2015;**117**:707-719.

53. Michl J, Park KC, Swietach P. Evidence-based guidelines for controlling pH in mammalian live-cell culture systems. *Commun Biol* 2019;**2**:144.
54. Sikkel MB, Francis DP, Howard J, Gordon F, Rowlands C, Peters NS, Lyon AR, Harding SE, MacLeod KT. Hierarchical statistical techniques are necessary to draw reliable conclusions from analysis of isolated cardiomyocyte studies. *Cardiovasc Res* 2017;**113**:1743-1752.
55. Tomek J, Hao G, Tomkova M, Lewis A, Carr C, Paterson DJ, Rodriguez B, Bub G, Herring N. beta-Adrenergic Receptor Stimulation and Alternans in the Border Zone of a Healed Infarct: An ex vivo Study and Computational Investigation of Arrhythmogenesis. *Front Physiol* 2019;**10**:350.
56. Robey IF, Baggett BK, Kirkpatrick ND, Roe DJ, Dosescu J, Sloane BF, Hashim AI, Morse DL, Raghunand N, Gatenby RA, Gillies RJ. Bicarbonate increases tumor pH and inhibits spontaneous metastases. *Cancer Res* 2009;**69**:2260-2268.
57. van Hasselt JGC, Rahman R, Hansen J, Stern A, Shim JV, Xiong Y, Pickard A, Jayaraman G, Hu B, Mahajan M, Gallo JM, Goldfarb J, Sobie EA, Birtwistle MR, Schlessinger A, Azeloglu EU, Iyengar R. Transcriptomic profiling of human cardiac cells predicts protein kinase inhibitor-associated cardiotoxicity. *Nat Commun* 2020;**11**:4809.
58. Takeishi Y. Pivotal roles of regulating the proline-rich tyrosine kinase 2 (PYK2) signaling in cardiac function and remodeling. *J Mol Cell Cardiol* 2014;**74**:295-296.
59. Takahashi T. Pyk2/CAKbeta signaling: a novel Ca(2+)-dependent pathway leading to cardiac hypertrophy. *J Mol Cell Cardiol* 2004;**36**:791-793.
60. Melendez J, Welch S, Schaefer E, Moravec CS, Avraham S, Avraham H, Sussman MA. Activation of pyk2/related focal adhesion tyrosine kinase and focal adhesion kinase in cardiac remodeling. *J Biol Chem* 2002;**277**:45203-45210.
61. Elliott AC, Smith GL, Eisner DA, Allen DG. Metabolic changes during ischaemia and their role in contractile failure in isolated ferret hearts. *J Physiol* 1992;**454**:467-490.
62. Lupu IE, De Val S, Smart N. Coronary vessel formation in development and disease: mechanisms and insights for therapy. *Nat Rev Cardiol* 2020.
63. Puente BN, Kimura W, Muralidhar SA, Moon J, Amatruda JF, Phelps KL, Grinsfelder D, Rothermel BA, Chen R, Garcia JA, Santos CX, Thet S, Mori E, Kinter MT, Rindler PM, Zacchigna S, Mukherjee S, Chen DJ, Mahmoud AI, Giacca M, Rabinovitch PS, Aroumougame A, Shah AM, Szweda LI, Sadek HA. The oxygen-rich postnatal environment induces cardiomyocyte cell-cycle arrest through DNA damage response. *Cell* 2014;**157**:565-579.
64. Neary MT, Ng KE, Ludtmann MH, Hall AR, Piotrowska I, Ong SB, Hausenloy DJ, Mohun TJ, Abramov AY, Breckenridge RA. Hypoxia signaling controls postnatal changes in cardiac mitochondrial morphology and function. *J Mol Cell Cardiol* 2014;**74**:340-352.
65. Chesler M, Kaila K. Modulation of pH by neuronal activity. *Trends Neurosci* 1992;**15**:396-402.
66. Nedergaard M, Kraig RP, Tanabe J, Pulsinelli WA. Dynamics of interstitial and intracellular pH in evolving brain infarct. *Am J Physiol* 1991;**260**:R581-588.

FIGURE LEGENDS

Figure 1: *Hearts recovering from cryo-infarction sustain an acidic interstitium and adapt with a change in pHi control that maintains a favourable intracellular acid-base milieu.* (A). Ventricular myocytes isolated from wild-type adult rats, imaged for pHi (cSNARF1) under superfusion with CO_2/HCO_3^- buffered Tyrode. Superfusate pH changed by varying [HCO_3^-]. Mean±SEM of 100-120 cells from 5 hearts. Best-fit line, pHi = 0.2469 pHe + 5.3093. (B). Exemplar image of metabolic response to cryo-infarction to left ventricle (LV) of adult rat. ^{13}C metabolic imaging performed 3 days after surgery shows increase in lactate and decrease in bicarbonate over a diffuse area of the myocardium, compared to sham-operated hearts. (C). Second series of cryo-infarction experiments on adult rat hearts, allowing up to 5 weeks of recovery after injury. At 2 weeks post-surgery, animals were injected with a mixture of pHLIP and Hoechst and hearts harvested for sectioning and imaging. Cryo-infarcted hearts retained a greater degree of pHLIP fluorescence across the myocardium, indicating a diffuse pattern of extracellular acidosis. Exemplar images shown. Scale bar 1.6 mm. (D). At 5 weeks post-injury, intracellular pH measured in beating hearts *in vivo* by ^{13}C MRI, from the ratio of $H^{13}CO_3^-$ to $^{13}CO_2$, compared to fluorescence (cSNARF1) measurements in superfused isolated myocytes. Mean±SEM from N=6, 9, 7 (from total of 150 cells), 6 (from total of 134 cells) hearts. Significant difference by two-way ANOVA (in vitro v in vivo and cryo v sham). (E). Frequency histogram of pHi measured for myocytes from cryo-infarcted or sham-operated hearts 5 weeks post-injury. N=150, 134 from 7 and 6 hearts, respectively. Hierarchical one-way ANOVA analysis, P=0.0007. (F). cSNARF-loaded myocytes isolated from myocardium 5 weeks post-injury stained with Hoechst *in vivo* according to local perfusion status. Analysis of nuclear Hoechst-33342 staining, showing an exemplar cell with no nuclear staining (i.e. originating from underperfused myocardial areas; green asterisk) and one with strong nuclear staining (i.e. derived from a well-perfused region; pink asterisk). (G). Correlation between nuclear Hoechst signal and resting pHi measured in the presence of CO_2/HCO_3^- buffer (Pearson's P=0.0118) or absence of CO_2/HCO_3^- buffer (P<0.0001). N=26-108 myocytes per bin, obtained from 6 hearts 5 weeks post-injury.

Figure 2: *In vivo acid-adapted cardiac myocytes manifest altered pHi regulation.* (A). Intrinsic buffering capacity measured by stepwise ammonium removal protocol in myocytes superfused with Hepes-buffered solutions. Data from 44 myocytes from 6 sham-operated hearts and 25 myocytes from 6 cryo-infarcted hearts. (B). NHE1 activity measured by ammonium prepulse using Hepes-buffered solutions. Data from 54 myocytes from 6 sham-operated hearts and 25 myocytes from 6 cryo-infarcted hearts. (C). NBC activity measured by ammonium prepulse using CO_2/HCO_3^- buffered solutions. Data from 74 myocytes from 6 sham-operated hearts and 30 myocytes from 6 cryo-infarcted hearts. (D). CBE activity measured by acetate prepulse using CO_2/HCO_3^- buffered solutions, with a 2 min interval in chloride-free solution to stabilise CO_2/HCO_3^- buffering prior to CBE activation. Data from 91 myocytes from 6 sham-operated hearts and 36 myocytes from 6 cryo-infarcted hearts. Significance testing by hierarchical two-way ANOVA shows significant effect of infarction (vs sham) on NHE1 (P<0.01) and CBE (P<0.01) activities, in addition to a significant effect of pH (P<0.001). (E). Western blots for NHE1, showing expression in lysates prepared from sham-operated, cryo-infarcted and non-operated, wild-type (WT) hearts in cohort 1

and sham-operated and cryo-infarcted hearts in cohort 2. Densitometric analysis of NHE1 expression, showing significant increase in NHE1 levels in cryo-injured hearts (n=2 in cohort 1; 4 in cohorot 2) relative to sham-operated hearts (n=2; 4; P=0.0401; determined by nested ANOVA) (F). Western blot for NHE1, showing expression in lysates from mice given a course of oral bicarbonate versus controls. Densitometric analysis, showing significant difference (P<0.05; determined by t-test).

Figure 3: *In vitro acid-adaptation of neonatal ventricular myocytes remodels pHi regulation through a shift in gene expression favouring acid-extruders.* (A). High-throughput imaging of pHi in cultured neonatal rat ventricular myocytes (NRVMs). Scale bar is 200 μm. Image analysis pipeline produces a statistical distribution of pHi. (B). Steady-state pHi measured over a range of pHe varied acutely by changing medium [HCO_3^-]. Relationship was mapped following 4 h equilibration in media containing 30 μM cariporide or in low-chloride media. Experiments performed on control myocytes (incubated at pHe=7.4 for 48 h) or acid-adapted myocytes (incubated at pHe=6.4 for 48 h). Significant alkaline shift for matching conditions by two-way ANOVA (P<0.01). Mean±SEM of the average value from 4 biological repeats (isolations), each performed with 4 technical replicates. In all panels, experiments were paired from the same isolation batch. (C). pHe-pHi relationship for myocytes adapted to pHe 6.4, 7.4 or 7.7 for 48 h. Mean±SEM of the average value from 3 biological repeats (isolations), each performed with 4 technical replicates. (D). pHe-pHi relationship for myocytes adapted to pHe 6.9 or 7.4 for 48 h. Mean±SEM of the average value from 8 biological repeats (isolations), each performed with 4 technical replicates. Arrows illustrate the iterative process that myocytes experience in low pHe: initial thermodynamically-driven pHi acidification, followed by a gradual re-active adaptation. (E). Histograms of pHi from an exemplar experiment from D. (F). Acid-extrusion flux measured by ammonium prepulse in CO_2/HCO_3^- buffered superfusates on control and acid-adapted myocytes. Mean±SEM of 496/602 cells from 8 isolations. Significant effect of acid-adaptation by hierarchical two-way ANOVA. (G). Acid-loading flux measured by acetate prepulse in CO_2/HCO_3^- buffered superfusates on control and acid-adapted myocytes (with a 2 min resting period in chloride-free solutions before activation of transport). Mean±SEM of 802/1013 cells from 8 isolations. Significant effect of acid-adaptation by hierarchical two-way ANOVA. (H). Analysis of RNAseq experiment on myocytes incubated for 48 h at five levels of pH between pH 6.4-7.4 (triplicates per condition). Genes belonging to “intracellular pH regulation” gene ontology GO:0051453. Analysis by DESeq2 shows significant correlation between medium pH and *Slc4a2* (positive), *Slc4a7* (negative) and *Slc9a1* (negative) transcripts. (I). Western blot showing upregulation of NHE1 and downregulation of AE2 in acid-adapted cells.

Figure 4: *Acid-adaptation of pHi control is a slow-onset process triggered by an intracellular H^+ sensor.* (A). Steady-state pHi measured over a range of pHe varied acutely in CO_2/HCO_3^- buffered media by changing [HCO_3^-]. Experiments performed on myocytes exposed for 4 h to low pHe (6.4), and compared to time-matched controls at pH 7.4. No significant effect of 4 h acid treatment. Mean±SEM of the average value from 3 biological repeats (isolations), each performed with 4 technical replicates. Experiments were paired from the same isolation batch. (B). pHe-pHi curves mapped in CO_2/HCO_3^- buffered media after 48 h of acid-adaptation (or control pHe) in the

presence or absence of CO_2/HCO_3^-. No significant effect of removing CO_2/HCO_3^- during adaptation. Mean±SEM of the average value from 3 biological repeats (isolations), each performed with 4 technical replicates. Experiments were paired from the same isolation batch. (C). pHi measured in low or normal chloride media following a 48 h period of acid-adaptation or control in low or normal chloride media. All experiments performed in presence of CO_2/HCO_3^-. Mean±SEM of the average value from 3 biological repeats (isolations), each performed with 4 technical replicates. Experiments were paired from the same isolation batch. (D). qPCR measurements of *Slc9a1* following 48 h acid-adaptation or time-matched controls in low or normal chloride media. Mean±SEM of the average value from 4 biological repeats (isolations). Experiments were paired from the same isolation batch.

Figure 5: *Acid-adaptation of pHi control is transduced by FAK-family H^+ sensors.* Steady-state pHi measured over a range of pHe varied acutely in CO_2/HCO_3^- buffered media by changing [HCO_3^-]. Experiments performed on acid-adapted myocytes (48 h in pH 6.4) or control myocytes (48 h in pH 7.4). Each biological repeat was performed with 4 technical repeats, and experiments were paired from the same isolation batch. (A). Effect of 10 µM SAHA. No significant effect. Mean±SEM of the average value from 3 biological repeats (isolations). (B). Effect of removing insulin-transferin-selenium (ITS). No significant effect. Mean±SEM of the average value from 3 biological repeats (isolations). (C). Effect of 10 µM PF-431396 (FAK1/Pyk2 inhibitor) included during 48-h acid-adaptation or control incubation. Significant effect of inhibitor ($P<0.001$) and significant interaction with incubation pH ($P<0.01$) on three-way ANOVA. Mean±SEM of the average value from 3 biological repeats (isolations). (D). When added for final 4 h period of acid-treatment and during imaging, PF-431396 had no significant effect. Mean±SEM of the average value from 3 biological repeats (isolations). (E). Effect of 100 nM Dasatinib during acid-adaptation (or time matched controls). No significant effect. Mean±SEM of the average value from 3 biological repeats (isolations). (F). Effect of 10 µM Bosentan during acid-adaptation (or time matched controls). No significant effect. Mean±SEM of the average value from 3 biological repeats (isolations). (G). Western blot showing downregulation of NHE1 in cells with the addition of 10 µM PF-431396 (FAK1/Pyk2 inhibitor) in acid-adaptation or control incubation cells. Effect of drug tested by two-way ANOVA; significant effect of drug (mean of three blots).

Figure 6: *Acid triggers change in FAK-family phosphorylation.* (A). Immunoblot for Pyk2 phosphorylation at Y402 and Y579/580, and total Pyk2 in lysates prepared after 10 min, 30 min or 48 h of incubation at pH 6.4 (or time-matched for pH 7.4 as control). Exemplar blot from three biological repeats. (B). Immunoblot for FAK1 phosphorylation at Y397 and Y576/577, and total FAK1 in lysates prepared after 10 min, 30 min or 48 h of incubation at pH 6.4 (or time-matched for pH 7.4 as control). Exemplar blot from three biological repeats. Densitometric quantification of blots from three independent isolations and treatment protocols. Two-way ANOVA tested for effect of pH.

FIGURE 1

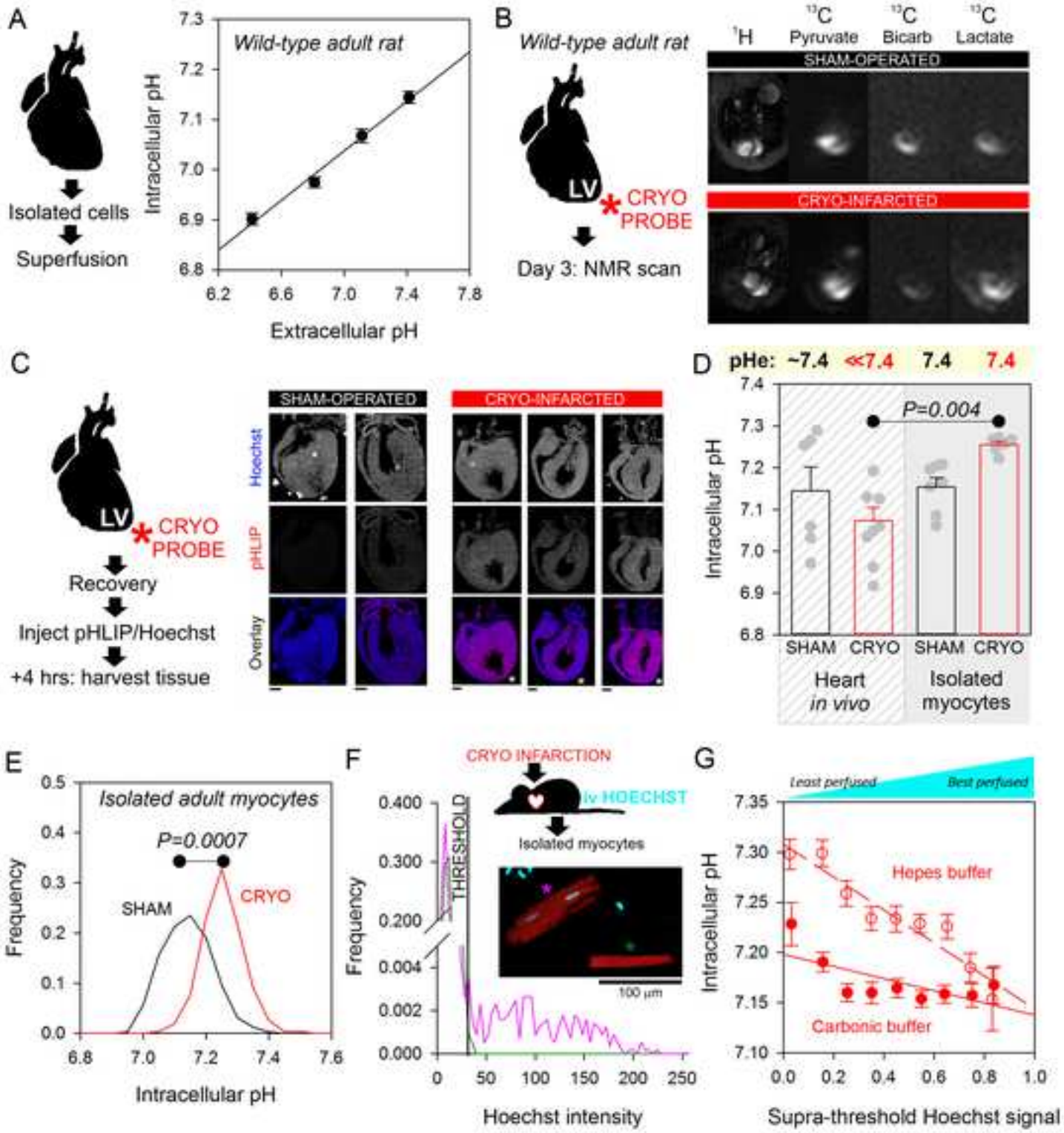

FIGURE 2

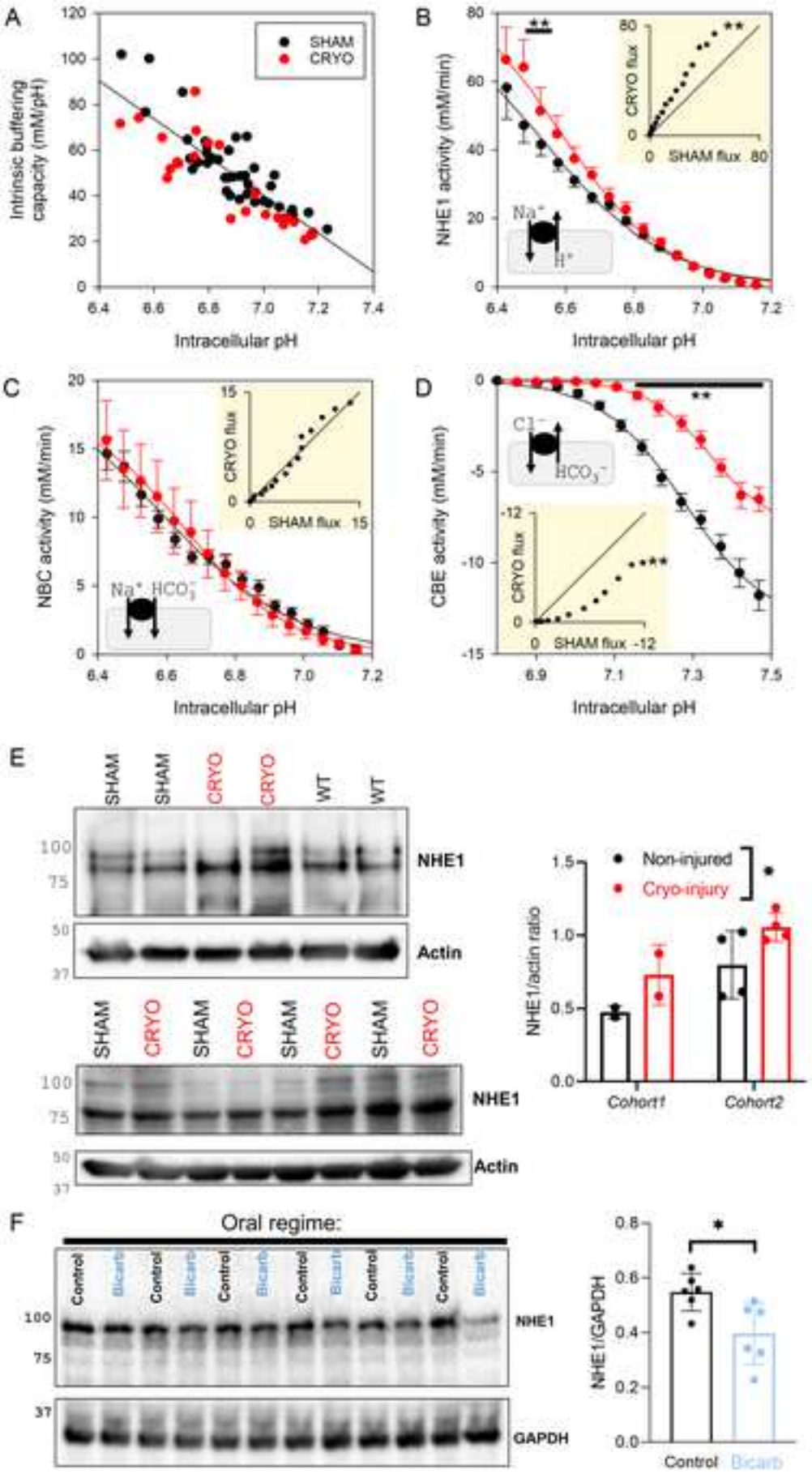

FIGURE 3

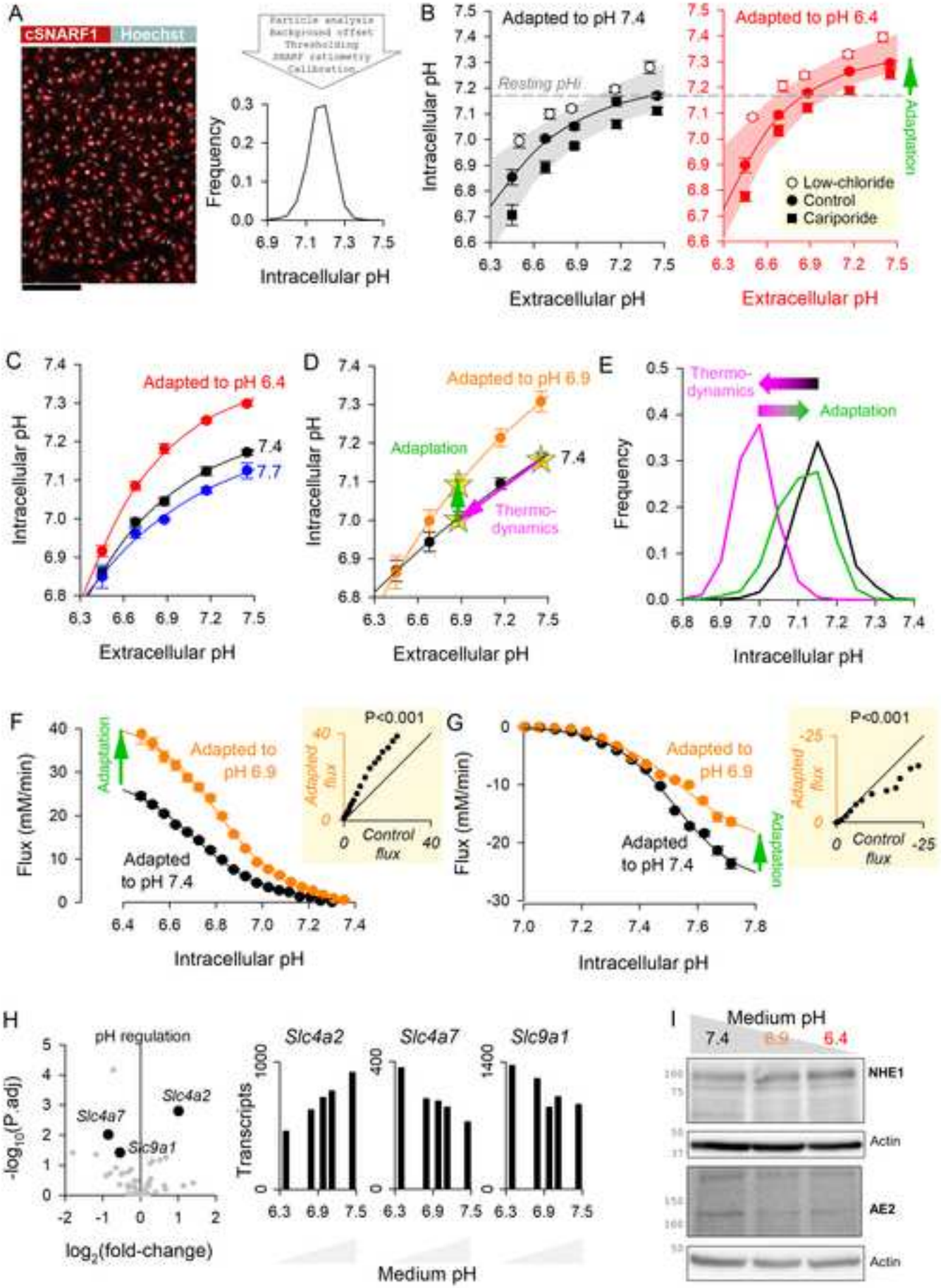

FIGURE 4

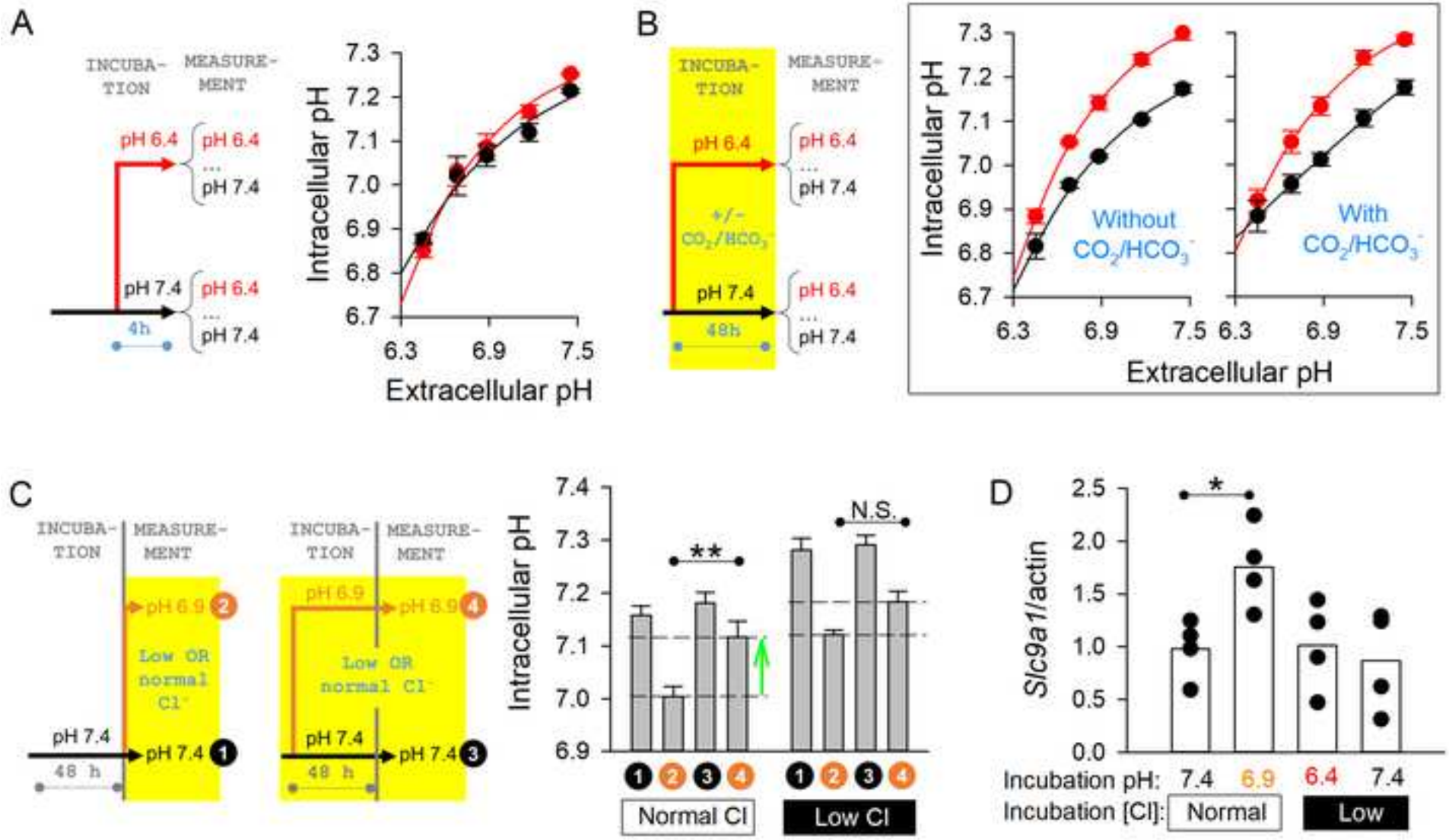

FIGURE 5

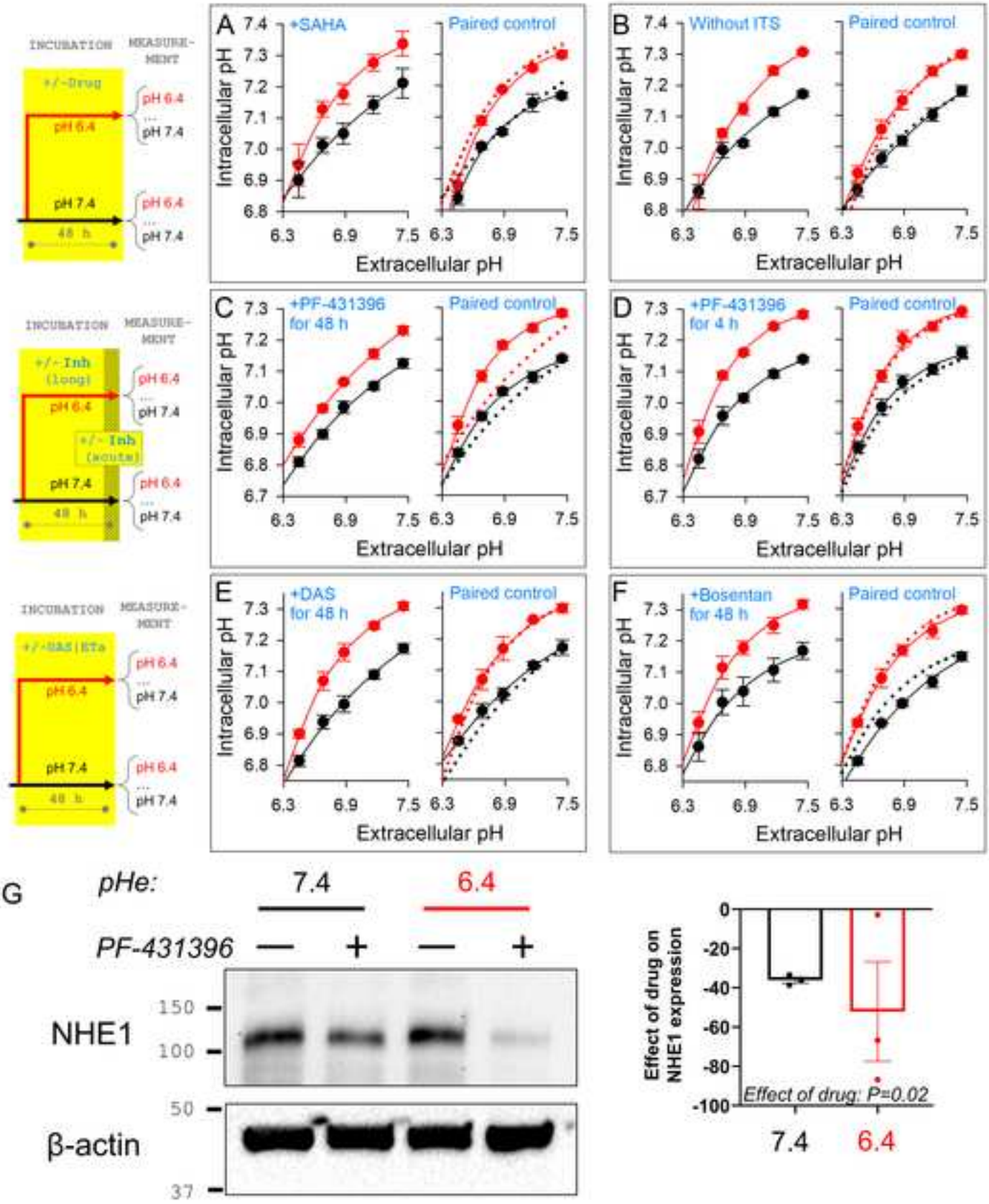

FIGURE 6

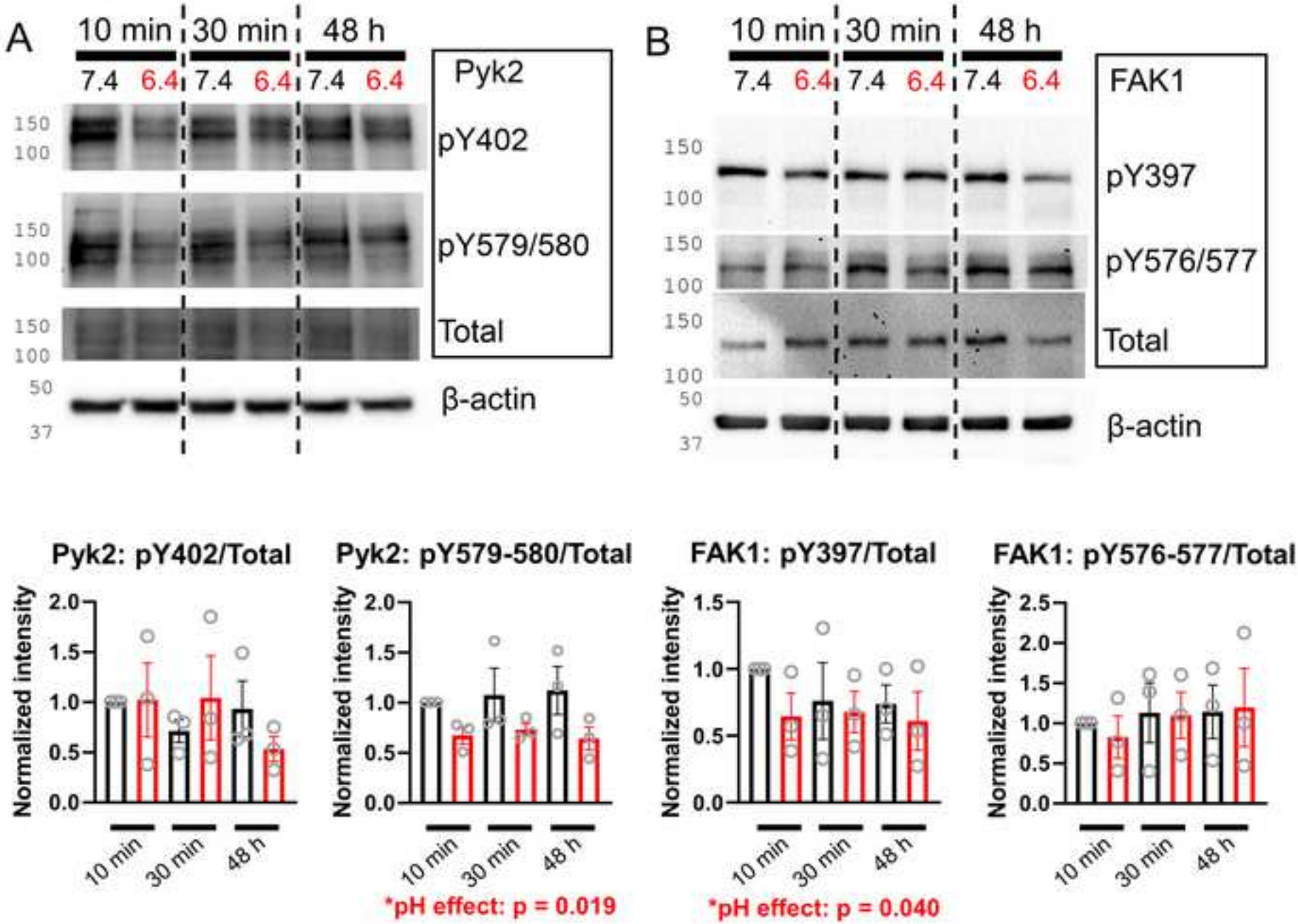

Graphical Abstract